Microcirculating System for Simultaneous Determination of Raman and Absorption Spectra of Enzymatic Reaction Intermediates and Its Application to the Reaction of Cytochrome *c* Oxidase with Hydrogen Peroxide

Denis A. Proshlyakov,[‡] Takashi Ogura,[‡,§] Kyoko Shinzawa-Itoh,[||] Shinya Yoshikawa,[||] and Teizo Kitagawa*[,‡,§]

Graduate University for Advanced Studies and Institute for Molecular Science, Okazaki National Research Institutes, Myodaiji, Okazaki, 444 Japan, and Department of Life Science, Faculty of Science, Himeji Institute of Technology, 1479-1 Kanaji, Kamigoricho, Akogun, Hyogo 678-12, Japan

Received May 24, 1995; Revised Manuscript Received October 23, 1995[⊗]

ABSTRACT: A new high-performance device for Raman/absorption simultaneous determination was developed. This was combined with a newly designed microcirculating system and was successfully applied to study intermediates in the reaction of bovine oxidized cytochrome *c* oxidase (CcO) with hydrogen peroxide under steady state conditions at ambient temperatures. Measurements with this device made it possible to correlate directly the species defined in terms of the visible absorption characteristics with specific Raman bands. The "607 nm" form of the enzyme obtained with $H_2{}^{16}O_2$ gave an oxygen isotope sensitive band at 804 cm^{-1} (769 cm^{-1} with $H_2{}^{18}O_2$) in the Soret excited resonance Raman (RR) spectrum. Its frequency and isotopic frequency shifts are exactly the same as those observed previously with 607 nm excitation in nonsimultaneous measurements for the 607 nm form, for which the presence of an oxoiron heme was demonstrated. The so-called "580 nm" form of the enzyme obtained with $H_2{}^{16}O_2$ gave the main oxygen isotope sensitive band at 785 cm^{-1} (750 cm^{-1} with $H_2{}^{18}O_2$) but appeared to consist of multiple species. This band was assigned to the Fe^{IV}═O stretching mode of ferryloxo heme on the basis of its isotopic frequency shift. Another oxygen isotope sensitive band was found at 355 cm^{-1} (340 cm^{-1} for $H_2{}^{18}O_2$), similar to the case of dioxygen reaction. Temporal behavior of this band did not agree with either that of the 804 cm^{-1} band or that of the 785 cm^{-1} band but seemed to grow between the two species. The RR spectra in the higher frequency region of the 607 nm and 580 nm forms excited at 427 nm were quite alike and did not support the formation of a porphyrin π-cation radical.

Cytochrome *c* oxidase (CcO)[1] (EC 1.9.3.1) is a terminal oxidase of a respiratory chain of aerobic organisms and catalyzes reduction of molecular oxygen to water coupled with proton translocation across mitochondrial inner membranes (Wikstrom et al., 1981; Chan & Li, 1990; Babcock & Wikstrom, 1992). The enzyme contains four redox active metal centers organized in two functionally distinct groups; the cytochrome *a* moiety consists of heme A (Fe_a) and Cu_A and participates in the electron transfer from cytochrome *c* to the catalytic site, while the cytochrome a_3 moiety consists of heme A (Fe_{a3}) and Cu_B and serves as the catalytic site for dioxygen reduction.

The information on the reaction mechanisms of CcO was first obtained from the low-temperature (Chance et al., 1975a,b; Clore et al., 1980a,b) and time-resolved (Gibson & Greenwood, 1963; Hill & Greenwood, 1984; Orii, 1988; Oliveberg et al., 1989; Verkhovsky et al., 1994) optical absorption and EPR (Hansson et al., 1982; Blair et al., 1985; Witt & Chan, 1987) experiments. However, it was hard to identify structurally the oxygen adducts generated at the Fe_{a3} center with these techniques. Recently, resonance Raman (RR) spectroscopy has been applied to investigate mechanisms of dioxygen reduction by CcO and identified the primary intermediate as a dioxy adduct of Fe_{a3} with the $Fe^{III}-O_2^-$ stretching mode (ν_{Fe-O_2}) at 571 cm^{-1} and the final one as the hydroxy adduct with the Fe^{III}−OH stretching mode (ν_{Fe-OH}) at 450 cm^{-1} (Varotsis et al., 1993; Han et al., 1990; Ogura et al., 1993). However, for three other oxygen isotope sensitive bands which were observed at 804 cm^{-1} (Ogura et al., 1993), 786 cm^{-1} (Ogura et al., 1993; Han et al., 1990; Varotsis et al., 1993), and 356 cm^{-1} (Ogura et al., 1993; Varotsis et al., 1993), their structural assignments as well as the position in the reaction sequence are currently under debate. These bands are expected to arise from "peroxy" and "ferryl" intermediates lying between the dioxy and hydroxy forms in the reaction cycle.

It was demonstrated recently that the peroxy and ferryl intermediates were generated in the reversal of the enzymic reaction in isolated mitochondria energized with ATP (Wikstrom & Morgan, 1992) and also in subjection of the oxidized enzyme to the reaction with hydrogen peroxide (Bickar et al., 1982; Kumar et al., 1984; Wrigglesworth, 1984; Gorren et al., 1986; Vygodina & Konstantinov, 1988). The species with a higher oxidation state (peroxy form) is characterized by the main peak at 607 nm, with a shoulder at 570 nm in the difference absorption spectrum, and is called the "607 nm" form (Vygodina & Konstantinov, 1988; Vygodina et

* Author to whom correspondence should be addressed.
[‡] Graduate University for Advanced Studies, Okazaki National Research Institutes.
[§] Institute for Molecular Science, Okazaki National Research Institutes.
[||] Himeji Institute of Technology.
[⊗] Abstract published in *Advance ACS Abstracts,* December 15, 1995.
[1] Abbreviations: RR, resonance Raman; EPR, electron paramagnetic resonance; CcO, cytochrome *c* oxidase.
[2] The recent time-resolved Raman experiments demonstrated that the 804 cm^{-1} species in fact developed prior to the 786 cm^{-1} species (Ogura et al., submitted).

0006-2960/96/0435-76$12.00/0 © 1996 American Chemical Society

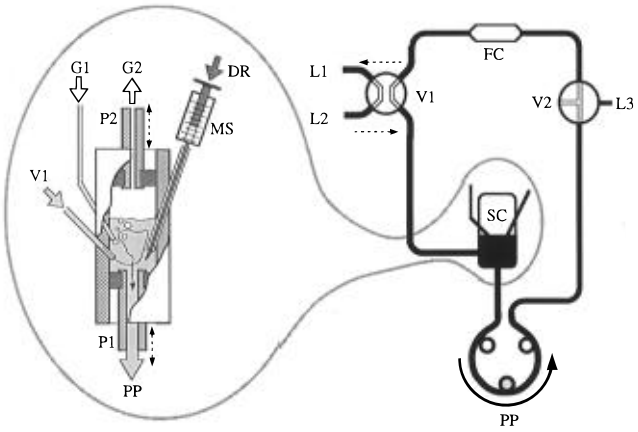

FIGURE 1: Schematic diagram of the microcirculating system. At right is a whole system: SC, sample container (details are illustrated at the left); PP, peristaltic pump; FC, flow cell; V1 and V2, valves; and L1, L2, and L3, inlet/outlet lines of solution. The system is shown for "measure" mode of V1. At left is an expanded illustration of the sample container: V1, from the flow cell; P1 and P2, hollow plungers; PP, to peristaltic pump; G1 and G2, gas inlet and outlet, respectively; MS, microsyringe; and DR, speed-controlled drive.

al., 1993; Weng & Baker, 1991). Another spectral form (ferryl form) has a characteristic peak at 580 nm with a minor band at 530 nm and accordingly is called the "580 nm" form. This species is thought to follow the 607 nm form in the reaction sequence toward water and to have a ferryloxo structure of Fe_{a3} (Witt & Chan, 1987). It has long been a subject of discussion whether these two intermediates in the reaction of CcO with H_2O_2 are the same as those involved in the reaction of CcO with O_2 (Orii, 1988; Vygodina & Konstantinov, 1988).

In order to solve this problem, we have applied RR spectroscopy to identify structures of oxygen adducts of Fe_{a3} of intermediates defined in terms of the absorption maxima. Previously, Ogura and Kitagawa (1988) constructed a device for simultaneous observation of Raman and absorption spectra of the same volume of a sample and successfully applied it to study the reaction of CcO with O_2 (Ogura et al., 1989, 1990a,b), but in this study, we have developed a new method applicable to a much smaller volume of sample and increased its performance significantly. To measure Raman spectra of the intermediates for such a slow reaction as that between resting CcO and H_2O_2, a steady state approach has been developed. In this paper, we explain the new method first and then its successful application to reaction intermediates of CcO with H_2O_2. The three oxygen isotope sensitive bands observed here have the same frequencies and oxygen isotope shifts as those observed for the reaction of reduced CcO with O_2.

EXPERIMENTAL PROCEDURES

Microcirculating System. To keep a concentration of reaction intermediates constant for a certain period, a new sample circulation system which allows continuous addition of a substrate during the measurements was constructed. This is illustrated in Figure 1. The enzyme solution derived from the sample container (SC) by a peristaltic pump (PP, i.d. = 1.5 mm, l = 140 mm, Tygon, Master Flex) comes to the flow cell (FC) through Teflon tubes (i.d. = 0.4 mm, total length = 50 cm). The linear flow rate at the sample point (0.6×0.6 mm^2 rectangular quartz flow cell) was about 2.8 m s^{-1}. It takes 1.5 s for a molecule to circulate the whole system under the present conditions.

To wash carefully the entire system, an X-type valve (V1) is incorporated at the outlet of the flow cell. Upon switching from "measure" mode to "wash" mode (broken lines in Figure 1), valve V1 is turned by 90° to connect the inlet of the sample container to that of distilled water through line L2 and the outlet of the flow cell to the waste container through line L1. In the wash mode [the flow direction is shown by dashed arrows in Figure 1 (right)], pumping water through the system (20−30-fold excess) washes all the components used in the measure mode. Another valve (V2, T-type), which is located before the flow cell, is used for calibration of the Raman shift. While valve V1 stays in the wash mode, acetone, acetonitrile, or ethanol is introduced into the flow cell as a secondary standard of Raman shifts via line L3 and valve V2.

The structure of the sample container is delineated in detail at the left in Figure 1. It consists of a thick-wall acrylic tube with two plungers (P1 and P2), which foot the outer tube with rubber seals. The bottom plunger (P1) is directly connected to the inlet of the peristaltic pump (PP) and forms a path for the solution to flow from the container to the cell. The outlet of the cell via valve V1 is connected to the thin stainless steel tube (surgery needle was used, i.d. = 0.9 mm, o.d. = 1.1 mm) which penetrates the wall of the container and returns the solution to the initial point. Another thin tube penetrating the wall of the container is the gas inlet (G1). When the experiment requires control of the gas phase (O_2, N_2, CO, etc.), line G1 can be used to incorporate a desired gas and plunger P2 serves as an outlet for the gas.

Sample Preparations. Bovine heart cytochrome *c* oxidase was purified as described previously (Yoshikawa et al., 1977). The enzyme solution in 10 mM sodium phosphate buffer (pH 7.2) was concentrated to about 500 μM (in terms of cytochrome aa_3) with an Amicon concentrator and stored either on ice or in liquid nitrogen until it was used. For the measurements, the enzyme solution was diluted with 100 mM sodium phosphate or borate buffer with desired pH as noted in the figure legends. $H_2{}^{16}O_2$ (30%, Wako Chemicals, Osaka, Japan) was used as purchased, while $H_2{}^{18}O_2$ was synthesized previously (Hashimoto et al., 1984). The stock solutions of hydrogen peroxide were made 100 or 50 mM and were kept frozen until the use.

Measurements of Spectra. In the present experiments, ca. 0.9 mL of the enzyme solution was introduced into the microcirculating system. The absorption spectrum of the resting enzyme was measured for 2 min and memorized as a reference. In the subsequent measurements, a difference spectrum against the resting enzyme was monitored. The reaction was initiated by rapid addition of different amounts of stock solution of hydrogen peroxide. Immediately after this, slow addition of another portion of hydrogen peroxide was started using a microsyringe (MS in Figure 1) and continued over the period of spectral accumulation. The microsyringe was fixed with a holder so that its needle could be in the solution, and the plunger of the microsyringe was driven at a controlled speed by OptMike Drive (DR, Sigma Koki) mounted on the same holder. The measurements were carried out at ambient temperature without gas phase control.

Raman/Absorption Simultaneous Measurements. To monitor the absorption and Raman spectra simultaneously for the same volume of a sample, a "high-performance Raman/

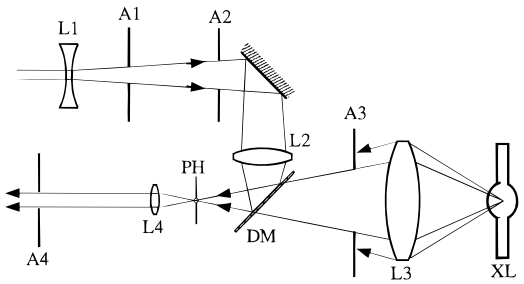

FIGURE 2: Light-mixing device: L1, L2, L3, and L4, lenses; A1, A2, A3, and A4, apertures; PH, pinhole (diameter = 25 μm); and DM, dichroic mirror. White light is obtained from a xenon lamp (XL), and laser light is introduced through aperture A1. The beam diameter at L2 is ca. 10 mm. For alignment of apertures A4 and A3 and lenses L4 and L3 to an identical optical axis, red laser light was passed in opposite to the white light, i.e. from aperture A4 to lens L3 through the pinhole and the dichroic mirror. Simultaneously, blue laser light was allowed to illuminate lens L2 from aperture A1. After apertures A1 and A2 were aligned to the optical axis of lens L2, they were fixed and used for subsequent alignment of the incoming laser beam. Finally, the position of the dichroic mirror was adjusted while the two beams after aperture A4 were monitored.

absorption simultaneous determination technique" was worked out in this study. Spatial mixing of laser light with white light takes place in the "light-mixing device" illustrated in Figure 2. The incoming laser light passes through two apertures (A1 and A2) and the focusing lens (L2, $f = 50$mm). Lens L2 focuses the laser beam to the 25 μm pinhole (PH) after reflection by a dichroic mirror (DM). The white light emitted from a xenon arc lamp (XL) (Hamamatsu Photonics, 30 W) is focused by camera lens L3 ($f = 50$ mm, $F = 1.4$) to the same pinhole. Any visible light, the wavelength of which is shorter than 480 nm, is reflected by the dichroic mirror, while the remaining part in the white light passes it.

Two parameters are critical for correct mixing of lights. First, the laser beam should illuminate the whole area of the pinhole. Therefore, the diameter of the focused laser beam should be somewhat larger than that of the pinhole. In the present configuration, 60−80% of the laser intensity passed the pinhole. Second, the focusing angles of the two beams should be the same. In other words, both beams should illuminate the same area at the dichroic mirror. It was achieved through expansion of the laser light by a dispersing lens (L1) as illustrated in Figure 2. The diameter of the white light at the dichroic mirror was adjusted to that of the laser beam by aperture A3. The mixed light, which has passed the pinhole, was collimated to a parallel beam using a microscope objective lens (L4), passed through another aperture (A4), and directed to the sample point.

Sample Illumination Device. The sample illumination point is delineated in Figure 3. This point is located about 5 m away from the light-mixing point. In this distance, the mixed beam is spread to about 5 mm, but separate observations for white and laser light in front of aperture A1 indicated that they were coaxial and had the same diameter. The mixed light was focused with a camera lens (L1, Nikon, $f = 105$ mm) to the sample in the flow cell as shown in Figure 3. The volume of the sample illuminated by the mixed light was of nearly cylindrical shape ($d = 15-20$ μm, $l = 600$ μm), when it was monitored with a microscope (white light was visualized with diluted rhodamine 6G solution). Raman scattering from this cylindrical volume is collected at a right angle with a camera lens (L2, Nikon, f

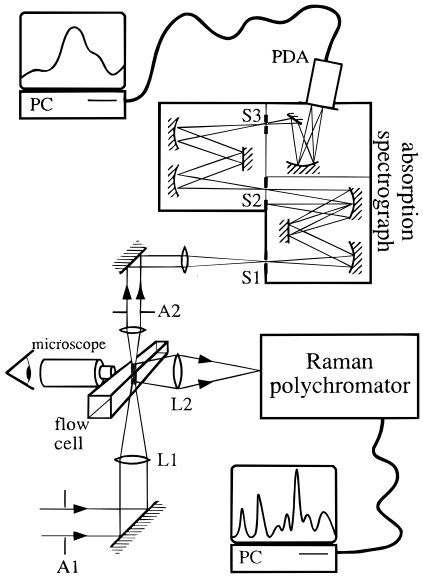

FIGURE 3: Schematic diagram of the experimental setup for Raman/absorption simultaneous measurements: A1 and A2, apertures; L1 and L2, lenses; S1, S2, and S3, slits of the triple monochromator for absorption measurements; PDA, photodiode array detector; and PC, personal computers. The cylindrical volume of the sample in the flow cell is exposed to the beam of the mixed light which is introduced from the device illustrated in Figure 2 through aperture A1. The diameter of aperture A1 was kept slightly smaller than that of the laser light in order to reject any white light which is not parallel to and/or extends over the laser beam. The laser light transmitted through the flow cell is rejected at slit S2 in the absorption monochromator.

= 50 mm, $F = 1.2$) and is focused onto the entrance slit of the polychromator (Ritsu Oyo Kogaku, DG-1000) which is equipped with an intensified photodiode array (Princetone Applied Research, 1421HQ) and controlled by a personal computer (PC).

The mixed light passed through the sample is reformed to a parallel beam and is directed to aperture A2 for elimination of the deviated part of the beam. This beam is then focused onto the entrance slit (S1) of the absorption monochromator (Jasco UV900) which consists of three stages. The first and second stages work as an optical filter which effectively rejects the laser light at slits S2 and S3. In the third stage, the light is dispersed and focused on the photodiode array (PDA) (C2327, Hamamatsu linear image sensor) controlled by another PC.

Raman Measurements. Raman scattering was excited at 427 nm. The exciting radiation was obtained by doubling the 854 nm output (2 W) of a Ti-sapphire laser (Spectra Physics, Model 3900), pumped by an Ar^+ ion laser (Spectra Physics, Model 2045), using $KNbO_3$ crystal. Laser power at the sample point was 2.5−7.5 mW, depending on the concentration of the enzyme. A holographic cutoff filter (430 nm) was used in front of the Raman polychromator. The resolution was ~1.0 cm^{-1} per channel, and the sensitivity of individual channels was normalized by division of the observed Raman spectrum by the spectrum of the white light. The Raman and absorption spectra were accumulated simultaneously, and the measurements were repeated several times for each isotope used. The data were acquired and processed with the XD Soft original program for IBM PC or NEC PC9800.

RESULTS

It was confirmed in this study that the 607 nm form is the main species in the steady state when bovine CcO was subjected to reaction with relatively low concentrations (below 100−200 μM) of H_2O_2 as reported for transient conditions (Wrigglesworth, 1984; Vygodina & Konstantinov, 1988). The preliminary absorption measurements indicated that, as the steady state concentration of peroxide increases, the 607 nm form was gradually replaced with the 580 nm form and the latter became dominant at millimolar concentrations of H_2O_2. High concentrations of enzyme (~50 μM) at neutral pH shifted the equilibrium toward the 607 nm form. In contrast, at high pH and low concentrations of the enzyme, the 607 nm form was easily converted to the 580 nm form, while the 607 nm form appears transiently. The actual distribution of the enzyme between 607 nm and 580 nm forms at given conditions (pH, enzyme concentration, and rate of peroxide addition) depended on the enzyme preparation. On the other hand, the spectral properties and pH-induced changes of the observed spectra scarcely depended on the enzyme preparations used. Therefore, for each preparation, a series of preliminary experiments were carried out to find an optimum concentration of H_2O_2 suitable to provide the desired form under given conditions. Since the observed spectral forms were reproducible but the amounts of H_2O_2 necessary to obtain them were not, the observed absorption spectra were used as criteria for specification of samples throughout this study.

Figure 4 depicts the low-frequency Raman (left) and visible absorption (right) spectra of CcO at a medium concentration of H_2O_2. To compare the spectra obtained under different conditions, the Raman intensities in the raw spectra were normalized by the porphyrin ν_7 band at 683 cm^{-1} which was assumed to be insensitive to the oxidation state and pH. Traces A and B show the Soret excited Raman spectra of the 607 nm form obtained with $H_2{}^{16}O_2$ and $H_2{}^{18}O_2$, respectively. These are distinct from the red-excited RR spectra of the 607 nm form reported previously (Proshlyakov et al., 1994). Trace C (= spectrum A − spectrum B) is the $H_2{}^{16}O_2$ − $H_2{}^{18}O_2$ difference spectrum (note the change in the intensity scales). Absorption spectrum C′ (difference spectrum with regard to the resting state), measured together with Raman spectra A and B, is compared with difference spectrum D, obtained under the same conditions but without laser illumination. The similarity between spectra C′ and D confirms that the reaction is not affected by laser illumination.

Traces C and C′ in Figure 4 represent the steady state difference Raman and difference absorption spectra, respectively, of the 607 nm form of CcO at neutral pH. The observed Raman spectrum is quite close to that reported for the dioxygen cycle at $\Delta t = 0.5$ ms (Ogura et al., 1993) except for the absence of the 571/544 cm^{-1} bands, which were assigned to the ν_{Fe-O_2} band of the dioxygen adduct (Han et al., 1990; Ogura et al., 1990a, 1993; Varotsis et al., 1989, 1990a). The Raman bands around 800 cm^{-1} in trace C can be resolved in two parts; the higher frequency components have the positive and negative peaks at 804 and 769 cm^{-1}, respectively, while the lower frequency components appear at 785 (positive) and 750 cm^{-1} (negative). Another oxygen isotope sensitive band appears at 355 cm^{-1}, with the corresponding negative band at 340 cm^{-1}. The 785/750 and 355/340 cm^{-1} difference peaks could not be recognized in the red-excited RR spectra (Proshlyakov et al., 1994).

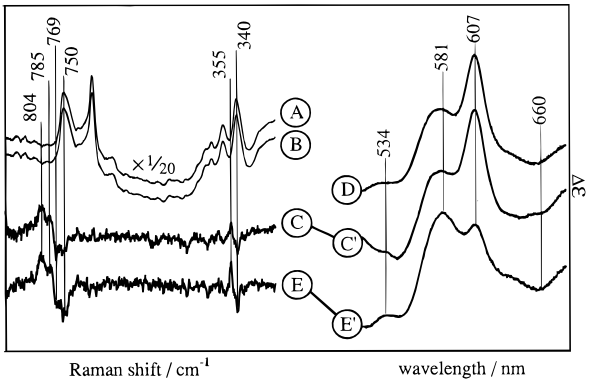

FIGURE 4: Steady state spectra of intermediates of oxidized cytochrome oxidase in the reaction with hydrogen peroxide. Raman spectra A and B were obtained with $H_2{}^{16}O_2$ and $H_2{}^{18}O_2$, respectively, at pH 7.4. Raman spectrum C represents the difference (spectrum C = spectrum A − spectrum B), and trace C′ shows the absorption spectrum measured simultaneously with spectra A and B. Absorption spectrum D was obtained under the same conditions as spectrum C′ but without laser illumination. Spectrum E denotes the differnce Raman spectrum observed at pH 8.5 (spectrum E = $H_2{}^{16}O_2$ derivative − $H_2{}^{18}O_2$ derivative), and absorption spectrum E′ was measured simultaneously with spectrum E. Intensities of Raman spectra were normalized with respect to the porphyrin ν_7 band at 683 cm^{-1}, and the ordinate full scale is 0.20. Traces A and B are multiplied by a factor of 0.05. Fluorescence background was subtracted digitally using a polynomial function, and the base line was made flat: excitation, 427 nm; laser power, 2.5 mW at the sample point; and resolution, ~1 cm^{-1} per channel. Accumulation time was 3 × 2250 and 1 × 2400 s for spectra C and E, respectively, for each isotope. Absorption spectra are represented as a difference with regard to the spectrum of the resting enzyme; ordinate full scale $\Delta\epsilon = 11.7$ mM^{-1} cm^{-1}. The pathlegnth is 0.6 mm. The sample contained 50 μM cytochrome oxidase for all spectra. See text about the steady state concentration of H_2O_2.

Traces E and E′ show the results obtained at pH 8.5 with a higher concentration of H_2O_2. In preliminary transient absorption experiments, there was no sharp pH dependent transition in the pH range between 7.4 and 8.5 with regard to spectral and kinetic properties of CcO in the reaction with H_2O_2, although some pH dependent changes took place. The difference Raman spectrum (E) is quite similar to that obtained at pH 7.4 (trace C), except for the intensity of the 355/340 cm^{-1} bands relative to those of the 804/769 and 785/750 cm^{-1} bands. However, the simultaneously observed absorption spectrum (trace E′) exhibits prominent differences. The band at 607 nm diminished significantly, and the band at 580 nm was developed instead. The fact that large changes in the absorption spectra are accompanied by small changes in the Raman spectra may imply that the Raman spectra arise from only the 607 nm form, but the 580 nm form gives rise to no oxygen isotope sensitive Raman bands. To clarify this point, relatively pure 607 nm and 580 nm forms were generated in a steady state by changing the concentrations of the enzyme and hydrogen peroxide.

Figure 5 depicts the Raman/absorption spectra of the 607 nm (traces A and A′) and 580 nm (traces B and B′) forms of CcO at pH 8.5. The absorption spectrum shown in trace A′ indicates that contamination of the 580 nm form is small, and in the corresponding RR spectrum (trace A), the bands at 804/769 cm^{-1} are more intense than the 785/750 cm^{-1} bands and the 355/340 cm^{-1} bands are twice as weak as those in trace B. When CcO was completely converted to the 580

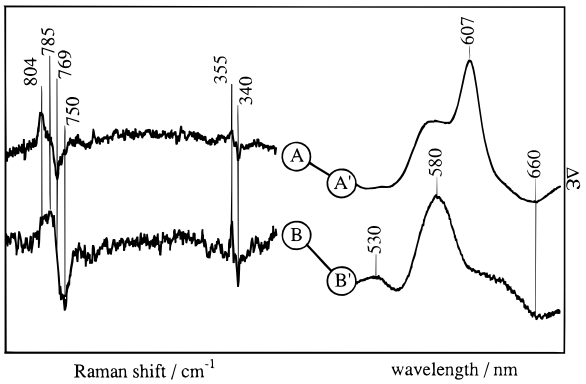

FIGURE 5: Steady state Raman/absorption spectra of the 607 nm and 580 nm forms of cytochrome oxidase at pH 8.5. Raman spectra A and B are shown as a difference of $H_2{}^{16}O_2$ compound minus $H_2{}^{18}O_2$ compound. Spectrum A/A′: laser power, 2.5 mW; accumulation time, 3 × 2400 s for each isotope; cytochrome oxidase concentration, 50 μM; and initial concentration of H_2O_2, 1 mM. Spectrum B/B′: laser power, 7.5 mW; accumulation time, 3 × 800 s for each isotope; cytochrome oxidase concentration, 10 μM; and initial concentration of H_2O_2, 5 mM. Ordinate scales and other conditions are the same as described in the legend to Figure 4. See text about the steady state concentration of H_2O_2.

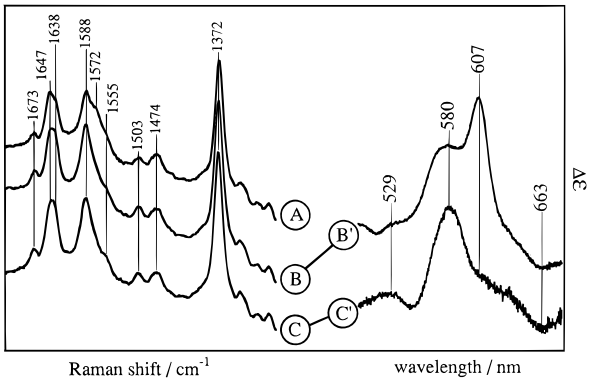

FIGURE 6: Steady state Raman spectra in the higher frequency region and simultaneously observed absorption spectra of resting cytochrome oxidase (A), the 607 nm form (B/B′), and the 580 nm form (C/C′) at pH 8.5. Spectra A and B/B′: laser power, 2.5 mW; accumulation time, 600 s and 1500 s, respectively; and cytochrome oxidase concentration, 30 μM. Spectrum C/C′: laser power, 5 mW; accumulation time, 900 s; and cytochrome oxidase concentration, 10 μM. All spectra were measured at pH 8.5, with $H_2{}^{16}O_2$ added for spectra B/B′ and C/C′. Spectrum C was normalized by the intensity of porphyrin ν_4 mode at 1372 cm^{-1} with respect to spectrum B, while spectra A and B were as observed. The ordinate full scale for difference absorption spectra is $\Delta\epsilon$ = 11.1 mM^{-1} cm^{-1}. Other conditions are the same as those described in the legend to Figure 4. See text about the steady state concentration of H_2O_2.

nm form as shown by trace B′ in Figure 5, the sharp symmetrical difference band at 804/769 cm^{-1} was replaced with broad bands around ∼785/∼750 cm^{-1}, and it appears as if several bands around 800−780/765−745 cm^{-1} were overlapped.

The Raman bands at 355/340 cm^{-1} are relatively stronger for the 580 nm form than for the 607 nm form. However, it is noted that the 355/340 cm^{-1} bands were observed for both 607 nm and 580 nm forms at the same frequency but with different intensities and the 355/340 cm^{-1} bands have never been observed alone. Although it might seem plausible to assume that the 580 nm form yields both the 785/750 and 355/340 cm^{-1} bands, their varied relative intensities were not compatible with the postulation that the two RR bands arise from a single intermediate. It is rather more reasonable to assume the presence of multiple species in the name of the 580 nm form besides the typical 607 nm form with RR bands at 804/769 cm^{-1}. To characterize these intermediates, RR spectra in the high-frequency region were examined.

Figure 6 shows the 1200−1700 cm^{-1} region of Raman spectra of resting CcO (A), the 607 nm form (B), and the 580 nm form (C). The RR spectrum of resting CcO (trace A) is in agreement with that reported (Varotsis et al., 1990b) with 427 nm excitation and contains more contributions from cytochrome *a* than from cytochrome a_3 because of the proximity of the excitation wavelength to its absorption maximum [the Soret maxima are located at 426 and 414 nm for cytochromes *a* and a_3, respectively (Vanesste, 1966; Sherman et al., 1991)]. The oxidation state marker band (ν_4) is observed at 1372 cm^{-1}, and the core-size marker band (ν_2) is located at 1572 cm^{-1} for high-spin cytohrome a_3 and at 1588 cm^{-1} for low-spin cytochrome *a*. The ν_{10} mode of cytochrome *a* appears at 1638 cm^{-1}, while the bands at 1647 and 1673 cm^{-1} arise from the formyl groups of cytochromes *a* and a_3, respectively.

The shift of the Soret absorption maximum to 427 nm for both 607 nm and 580 nm forms is likely to be ascribed to a change in cytochrome a_3. It is noted that the RR spectra of the 607 nm (trace B) and 580 nm forms (trace C) are quite alike and close to the low-spin spectrum of resting CcO. Disappearance of the high-spin RR bands during the reaction is due to changes in cytochrome a_3, and these changes are similar to those reported for the formation of "oxygenated" CcO (Babcock et al., 1981; Carter et al., 1981), though the latter is likely to be a mixture of several species. The close similarity of the observed RR spectra of the 607 nm, 580 nm, and resting forms suggests that they reflect mainly the cytochrome *a* moiety or that the RR spectrum of cytochrome a_3 in the reaction intermediates is not greatly different from that of oxidized cytochrome *a*. The latter alternative is more likely due to the following reasons.

The high-spin RR bands of resting cytochrome a_3 with the absorption maximum at 414 nm are observed upon excitation at 427 nm. The Soret maximum of cytochrome a_3 in the 607 nm form must be closer to 427 nm than that in the resting CcO, and therefore, no appearance of any RR bands of cytochrome a_3 of the 607 nm and 580 nm forms appears unnatural. In fact, RR spectra of compound II of HRP are close to those of ferric low-spin heme proteins (Ogura & Kitagawa, 1988; Paeng & Kincaid, 1988). The similarity of the position and intensity of the Soret absorption maximum of the 607 nm form to those of the 580 nm form (Weng & Baker, 1991), together with the absence of downshifted ν_2 and ν_{10} bands for the 607 nm form, indicates that the formation of a porphyrin π-cation radical for the 607 nm/804 cm^{-1} form of CcO is less likely.

DISCUSSION

Microcirculating System. The most serious problem in RR spectroscopy of intermediates of hemoproteins is low signal-to-noise (S/N) ratio of spectra. Generally, the accumulation time cannot be made long due to the limited amount of samples. In order to overcome this difficulty, the microcirculating system is introduced in this study. Its main advantages over the spinning cell, instead of which it was developed, are as follows: (1) The freedom of manipulations on the sample during the measurement allows for the

extension of accumulation time. (2) The Raman/absorption simultaneous determination technique can be applied, thus providing the real-time information on the changes in the sample. (3) It is free of mechanical fluctuations associated with the spinning cell, resulting in a higher quality spectrum. (4) Wavenumber calibrations can be performed more reliably. The first advantage allowed the addition of hydrogen peroxide to CcO at a constant rate during the reaction. This made it possible to maintain a steady state concentration of a given intermediate for 40−60 min.

Visible absorption spectroscopy has provided important information on the oxidation and coordination states of various heme proteins, including their reaction intermediates. Furthermore, it could be a sensitive tool for detection of possible photochemical damage induced by laser illumination. Therefore, it is desirable to monitor the absorption spectra of the portion of sample illuminated by laser light for Raman measurements. For this purpose, Ogura and Kitagawa (1988) constructed a device for Raman/absorption simultaneous measurements, but mixing of the laser and white lights in an optical fiber deprived the Raman excitation light of polarization property and lowered the quality of Raman spectra. In the present method, the excitation light remains to be polarized and, furthermore, the excitation beam can be focused to a diameter as small as 15 μm. These made the accumulation time of spectra significantly shorter, and higher spectral resolution can be achieved with a narrower beam. A tiny focused beam would result in a higher temporal resolution in its application to time-resolved experiments. The new technique adopted here is indispensable in the providing of new Raman information on transient species generated in the reaction of CcO with H_2O_2 and specified by visible absorption spectra.

The deviation of white and laser beams from full superposition at the sample point, if any, would be caused by distribution of intensity across the laser beam and dispersion of light at the lenses. To avoid this, the laser beam passes through three apertures on the way from source to the sample point, and each of them eliminates the edge part of the beam. To reduce further the light dispersion, a camera lens was used for focusing of the beam to the sample instead of an ordinary lens in the earlier version.

Intermediates of Cytochrome c Oxidase. The 607 nm form is known to be the primary intermediate formed in the reaction of H_2O_2 with resting CcO. It is two electrons above the oxidized enzyme (Wikstrom & Morgan, 1992) and was generally referred as the peroxy complex with a bridged [Fe−O−O−Cu] structure (Vygodina & Konstantinov, 1988; Vygodina et al., 1993). We have carried out transient absorption experiments and confirmed that no absorption band is developed at 580 nm prior to the rise of the 607 nm band (data not shown). We reported recently the red-excited Raman spectrum of a reaction intermediate of CcO in the reaction with H_2O_2 (Proshlyakov et al., 1994). This intermediate was identified as an oxo compound with the $\nu_{Fe=O}$ band at 803 cm^{-1}, whose oxygen atom is hydrogen bonded to the surrounding, and was suggested to correspond to the 607 nm form, although it was not proven by the simultaneous absorption measurements. The present study provides the conclusive evidence that the 803/769 cm^{-1} species arises from the 607 nm form and should be regarded as an oxo intermediate. In this respect, cytochrome oxidase behaves in a manner similar to that of peroxidases (Hashimoto et al., 1986; Ogura & Kitagawa, 1988; Paeng & Kincaid, 1988; Egawa et al., 1992).

The peroxy oxidation level of the enzyme should have an extra oxidative equivalent above the ferryloxo heme. This might be retained in the form of (a) a π-cation radical, like in horseradish peroxidase compound I (Paeng & Kincaid, 1988; Palaniappan & Terner, 1989; Chuang & Van Wart, 1992), (b) an amino acid radical, like in cytochrome *c* peroxidase compound ES (Yonetani et al., 1966; Sivaraja et al., 1989), or (c) Fe^V heme. The close similarity of the Soret absorption peaks between the 607 nm and 580 nm forms makes the possibility (a) unlikely, and moreover, it does not exhibit the RR spectral characteristics of a Fe^{IV}═O porphyrin π-cation radical (Kitagawa & Mizutani, 1994) as mentioned above. Possibility (b) cannot be ruled out for RR spectra, but no EPR signal assignable to an amino acid radical has been detected. The RR spectral properties of the Fe^V heme have not been reported yet and are under investigation in this laboratory.

In the reaction of CcO with O_2, five oxygen isotope sensitive bands were observed. The primary intermediate, assigned to an end-on type dioxy structure with $\nu_{Fe\text{-}O_2}$ at 571 cm^{-1}, is not expected to be developed in the reaction of resting CcO with H_2O_2. The final intermediate, identified as a hydroxy heme with the Fe−OH stretching RR band at 450 cm^{-1}, would exhibit rapid oxygen exchange with bulk water and thus would not give an oxygen isotope difference band in such a slow overall reaction as that between ferric CcO and H_2O_2. The assignments of three other oxygen isotope sensitive bands, found at 804, 785, and 355 cm^{-1}, to the peroxy and ferryl intermediates are under debate. In this study, we demonstrated that all three oxygen isotope sensitive bands appear in the reaction of ferric CcO with H_2O_2. We did not find distinct differences between intermediates of the two reactions either in their frequencies and band shapes or in the values of the shifts upon $^{16}O/^{18}O$ substitution. These data strongly suggest that the intermediates in both reactions are structurally identical.

The 580 nm absorption form of CcO is one oxidative equivalent lower than the 607 nm form (Wikstrom & Morgan, 1992). It suggests that the 580 nm form might exist in the ferryloxo state. In fact, the frequency (785 cm^{-1}) of the oxygen isotope sensitive Raman band arising from the 580 nm form is very close to the Fe^{IV}═O stretching frequency of many hemoproteins (Kitagawa & Mizutani, 1994). It exhibits a downshift by 35 cm^{-1} upon $^{16}O/^{18}O$ substitution as expected for Fe^{IV}═O stretching at 785 cm^{-1}.

Recently, Ogura et al. (submitted) demonstrated that the 356 cm^{-1} band is observed together with the 804 cm^{-1} band but not with the 786 cm^{-1} band. Varotsis et al. (1993) reported that the 356 cm^{-1} band precedes the 786 cm^{-1} band in the time course of the reaction and assigned it to the short-lived [Fe−O−O(H)] structure, but they failed to resolve the 804 and 786 cm^{-1} bands. The 356 cm^{-1} band is known to be insensitive to D_2O substitution, and $^{16}O^{18}O$ does not yield a new Raman band at intermediate frequencies (Ogura et al., 1993). The present results show that the intermediate giving rise to the 355 cm^{-1} band is quite stable and can be well-populated in the steady state reaction of ferric CcO with H_2O_2, in which the estimated overall rate is less than 1 s^{-1}. In the peroxide reaction, the band at 355 cm^{-1} is never seen alone and its behavior is rather close to that of the 785 cm^{-1}

band. Moreover, the 355 cm^{-1} band appears when the absorption spectrum indicates the 580 nm form.

The results shown here, together with behaviors of the three RR bands in the dioxygen reaction (Ogura et al., submitted), indicate that three RR bands arise from different intermediates. The observation that the 355/340 cm^{-1} bands appear kinetically between the 804/769 and 785/750 cm^{-1} bands suggests that the intermediate giving rise to the 355/340 cm^{-1} bands also has an oxoiron heme. This frequency is too low to assign it to the Fe═O stretching but is reasonable as the His-Fe═O bending mode. As described above, the RR band around 800 cm^{-1} became broader when the 355/340 cm^{-1} bands were prominent. Accordingly, it is reasonable to assume that the intermediate having the oxygen isotope sensitive band at 355 cm^{-1} is the third oxoiron species with the Fe═O stretching band around 800 cm^{-1} and its bending at 355 cm^{-1}.

Although this seems most reasonable at the present stage, the appearance of the third band around 800 cm^{-1} is not necessarily evident in the present observations, and therefore, we cannot rule out a possibility that the third species has the oxygen isotope sensitive band only at 355 cm^{-1}. In this case, this band might be assigned to a single bond Fe−O stretching, possibly of the Fe−O−O−H speices which might be generated upon oxidation of ferryloxo heme by H_2O_2. However, this frequency is still considerably lower than the Fe−O single bond stretching frequecies of the Fe−O_2 (571 cm^{-1}) and Fe−OH (450 cm^{-1}) compounds. An alternative explanation admits that two pathways exist for both peroxide and dioxygen reactions and that the 355 cm^{-1} species belongs to one while the 804 cm^{-1} and 785 cm^{-1} species belong to another pathway.

In conclusion, we have developed a new microcirculating system for simultaneous determination of Raman and absorption spectra and successfully applied it to the reaction of oxidized cytochrome oxidase and hydrogen peroxide. We have finally demonstrated that the 607 nm and 580 nm forms give 804 cm^{-1} and 786 cm^{-1} Raman bands, respectively, which are both assignable to Fe═O stretching vibrations of the reaction intermediates at peroxy and ferryl oxidation levels. We also show that the 355 cm^{-1} species is stable under ambient conditions and is mostly populated in the 580 nm form of the enzyme.

REFERENCES

Babcock, G. T., & Wikstrom, M. (1992) *Nature 356*, 301−309.

Babcock, G. T., Callahan, P. M., Ondrias, M. R., & Salmeen, I. (1981) *Biochemistry 20*, 959−966.

Bikar, D., Bonaventura, J., & Bonaventura, C. (1982) *Biochemistry 21*, 2661−2666.

Blair, D. F., Witt, S. N., & Chan, S. I. (1985) *J. Am. Chem. Soc. 107*, 7389−7399.

Carter, K. R., Antalis, T. M., Palmer, G., Ferris, N. S., & Woodruff, W. H. (1981) *Proc. Natl. Acad. Sci. U.S.A. 78*, 1652−1655.

Chan, S. I., & Li, P. M. (1990) *Biochemistry 29*, 1−12.

Chance, B., Saronio, C., & Leigh, J. S., Jr. (1975a) *J. Biol. Chem. 250*, 9226−9237.

Chance, B., Saronio, C., & Leigh, J. S., Jr. (1975b) *Proc. Natl. Acad. Sci. U.S.A. 72*, 1635−1640.

Chuang, W.-J., & Van Wart, H. E. (1992) *J. Biol. Chem. 267*, 13293−13301.

Clore, G. M., Andreasson, L.-E., Karlsson, B., Aasa, R., & Malmstrom, B. G. (1980a) *Biochem. J. 185*, 139−154.

Clore, G. M., Andreasson, L.-E., Karlsson, B., Aasa, R., & Malmstrom, B. G. (1980b) *Biochem. J. 185*, 155−167.

Egawa, T., Miki, H., Ogura, T., Makino, R., Ishimura, Y., & Kitagawa, T. (1992) *FEBS Lett. 305*, 206−208.

Gibson, Q. H., & Greenwood, C. (1963) *Biochem. J. 86*, 541−554.

Gorren, A. C. F., Dekker, H., & Wever, R. (1986) *Biochim. Biophys. Acta 852*, 81−92.

Han, S., Ching, Y.-c., & Rousseau, D. L. (1990) *Nature 348*, 89−90.

Hansson, O., Karlsson, B., Aasa, R., Vanngard, T., & Malmstrom, B. (1982) *EMBO J. 1*, 1295−1297.

Hashimoto, S., Tatsuno, Y., & Kitagawa, T. (1984) *Proc. Jpn. Acad., Ser. B 60*, 345−348.

Hashimoto, S., Teraoka, J., Inubushi, T., Yonetani, T., & Kitagawa, T. (1986) *J. Biol. Chem. 261*, 11110−11118.

Hill, B. C., & Greenwood, C. (1984) *Biochem. J. 218*, 913−921.

Kitagawa, T., & Mizutani, Y. (1994) *Coord. Chem. Rev. 135/136*, 685−735.

Kumar, C., Naqui, A., & Chance, B. (1984) *J. Biol. Chem. 259*, 11668−11671.

Ogura, T., & Kitagawa, T. (1988) *Rev. Sci. Instrum. 59*, 1316−1320.

Ogura, T., Yoshikawa, S., & Kitagawa, T. (1989) *Biochemistry 28*, 8022−8027.

Ogura, T., Takahashi, S., Shinzawa-Itoh, K., Yoshikawa, S., & Kitagawa, T. (1990a) *J. Am. Chem. Soc. 112*, 5630−5631.

Ogura, T., Takahashi, S., Shinzawa-Itoh, K., Yoshikawa, S., & Kitagawa, T. (1990b) *J. Biol. Chem. 265*, 14721−14723.

Ogura, T., Takahashi, S., Hirota, S., Shinzawa-Itoh, K., Yoshikawa, S., Appelman, E. H., & Kitagawa, T. (1993) *J. Am. Chem. Soc. 115*, 8527−8536.

Ogura, T., Hirota, S., Proshlyakov, D. A., Shinzawa-Itoh, K., Yoshikawa, S., & Kitagawa,T. *J. Am. Chem. Soc.* (in press).

Oliveberg, M., Brzezinski, P., & Malmstrom, B. G. (1989) *Biochim. Biophys. Acta 977*, 322−328.

Orii, Y. (1988) *Ann. N. Y. Acad. Sci. 550*, 105−117.

Paeng, K.-J., & Kincaid, J. R. (1988) *J. Am. Chem. Soc. 110*, 7913−7915.

Palaniappan, V., & Terner, J. (1989) *J. Biol. Chem. 264*, 16046−16053.

Proshlyakov, D. A., Ogura, T., Shinzawa-Itoh, K., Yoshikawa, S., Appelman, E. H., & Kitagawa, T. (1994) *J. Biol. Chem. 269*, 29385−29388.

Sherman, D., Kotake, S., Ishibe, N., & Copeland, R. A. (1991) *Proc. Natl. Acad. Sci. U.S.A. 88*, 4265−4269.

Sivaraja, M., Goodin, D. B., Smith, M., & Hoffman, B. M. (1989) *Science 245*, 738−740.

Vanesste, W. H (1966) *Biochemistry 5*, 838−848.

Varotsis, C., Woodruff, W. H., & Babcock, G. T. (1989) *J. Am. Chem. Soc. 111*, 6439−6440.

Varotsis, C., Woodruff, W. H., & Babcock, G. T. (1990a) *J. Am. Chem. Soc. 112*, 1297.

Varotsis, C., Woodruff, W. H., & Babcock, G. T. (1990b) *J. Biol. Chem. 265*, 11131−11136.

Varotsis, C., Zhang, Y., Appelman, E. H., & Babcock, G. T. (1993) *Proc. Natl. Acad. Sci. U.S.A. 90*, 237−241.

Verkhovsky, M. I., Morgan, J. E., & Wikstrom, M. (1994) *Biochemistry 33*, 3079−3086.

Vygodina, T. V., & Konstantinov, A. A. (1988) *Ann. N. Y. Acad. Sci. 550*, 124−138.

Vygodina, T. V., Schmidmaier, K., & Konstantinov, A. A. (1993) *Biol. Mem. 6*, 883−906.

Weng, L., & Baker, G. M. (1991) *Biochemistry 30*, 5727−5733.

Wikstrom, M., & Morgan, J. E. (1992) *J. Biol. Chem. 267*, 10266−10273.

Wikstrom, M., Krab, K., & Saraste, M. (1981) *Cytochrome Oxidase: A Synthesis*, Academic Press, New York.

Witt, S. N., & Chan, S. I. (1987) *J. Biol. Chem. 262*, 1446−1448.

Wrigglesworth, J. M. (1984) *Biochem. J. 217*, 715−719.

Yonetani, T., Schleyer, H., & Ehrenberg, A. (1966) *J. Biol. Chem. 241*, 3240−3243.

Yoshikawa, S., Choc, M. G., O'Toole, M. C., & Caughey W. S. (1977) *J. Biol. Chem. 252*, 5498−5508.

BI9511705